

# Towards the synthesis of sugar amino acid containing antimicrobial noncytotoxic CAP conjugates with gold nanoparticles and a mechanistic study of cell disruption†‡

Sudip Pal, Kalyan Mitra, Sarfuddin Azmi, Jimut Kanti Ghosh and Tushar Kanti Chakraborty\*

Received 3rd March 2011, Accepted 8th April 2011

DOI: 10.1039/c1ob05338h

Cationic antimicrobial peptides are potent inhibitors of growth of a broad spectrum of micro-organisms but often have large cytotoxic effects. We prepared some novel sugar amino acid containing cyclic cationic peptides and their Au nanoparticle attached counterparts and studied their antimicrobial activities and cytotoxic behaviour, including an investigation of the mechanism of the cytotoxicity.

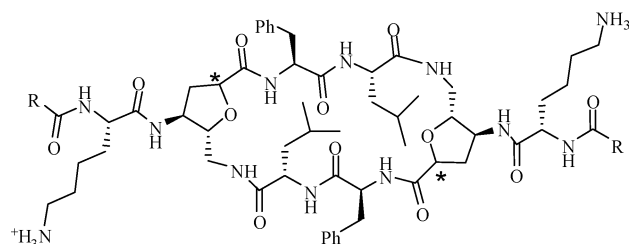
## Introduction

The development of new antibiotics with novel modes of action assumes great significance today due to the increasing emergence of bacterial resistance towards the existing antibiotics.<sup>1</sup> Cationic antimicrobial peptides (CAPs) – linear as well as cyclic – are considered as potential antibiotics but sometimes have significant toxic behaviour which curbs their application as antibiotics.<sup>2</sup> The mechanistic pathway of cell destruction by any antimicrobial substance may proceed through pore formation in the lipid bilayer by barrel stave, carpet or toroidal-pore mechanism or may penetrate into the cell to bind to crucial cell components.<sup>3</sup> For this, the size, chemical composition, amphipathicity and cationic charge of the peptide are important factors. Substances attached to a carrier may also have enhanced activities against microorganisms as compared to their native selves with lesser cytotoxic effect. One of the most discussed and used carriers to date one is the gold nanoparticle due to its nontoxicity, therapeutic effect and biocompatible unique optical and photothermal behaviour.<sup>4</sup>

Herein we report the synthesis of some sugar amino acid<sup>5</sup> containing novel cyclic cationic peptides **1–4** and their therapeutic and mechanistic study towards the disruption of various microbial cells.<sup>6</sup> They were also attached to gold nanoparticles to study their therapeutic effects and also to get an insight into the mechanistic pathway.

## Results and discussion

Peptides **1–4** were synthesized by cyclodimerization<sup>7</sup> of H<sub>2</sub>N-Saa(BocNH)-Phe-Leu-OH following our earlier reported procedure.<sup>6c</sup> Boc-deprotection of the resulting *cyclo*-[Saa-



- 1:** R = (CH<sub>2</sub>)<sub>2</sub>SH; \* = (S); **2:** R = (CH<sub>2</sub>)<sub>2</sub>SH; \* = (R);  
**3:** R = (CH<sub>2</sub>)<sub>5</sub>SH; \* = (S); **4:** R = CH<sub>2</sub>CH<sub>3</sub>; \* = (S);

(BocNH)-Phe-Leu], coupling with RCO-Lys(Boc)-OH and final deprotection gave the desired peptides.

Peptides **1–3** were attached to the gold nanoparticles through place exchange reaction with octanethiol stabilized gold nanoparticles and the resulting conjugates could be visualized in their TEM pictures taken in MeOH and aqueous solution of peptide **1** attached nanoparticles (Fig. 1). Peptide **1** attached to AuNP in MeOH and water was studied using TEM at 120 kV. Micrographs revealed homogeneous distribution of electron dense round particles without any aggregation in both MeOH and in water. The diameter of the particles ranged from 1.2 to 2.5 nm. Representative electron micrographs at magnifications of 265 000× are presented in Fig. 1.

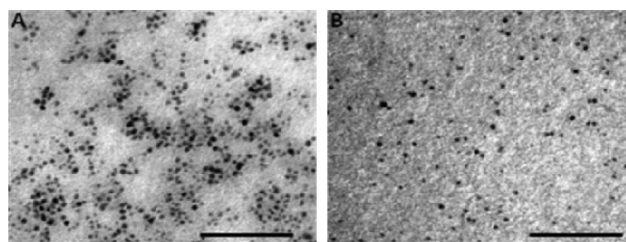


**Fig. 1** Transmission electron micrographs of peptide **1** attached to Au nano particles (A) in MeOH solution and (B) in water. Bar represents 50 nm.

CSIR-Central Drug Research Institute, Lucknow 226001, India. E-mail: chakraborty@cdri.res.in

† CSIR-CDRI Communication No. 8040

‡ Electronic supplementary information (ESI) available. See DOI: 10.1039/c1ob05338h

Peptide **4** was prepared to investigate two subjects. One was the importance of the thiol group in the peptide for its attachment to the gold nanoparticles as there are reports<sup>8</sup> where the electrostatic attraction of the ammonium group is the key factor for the attachment of the peptide to the gold nanoparticles and the other is the effect of the thiol group over that of the alkyl groups towards the antimicrobial activities of the peptides.

When peptide **4** was incubated with gold nanoparticles under the same conditions as the other peptides, its inability to attach itself to gold was clearly visible (Fig. 2A) when compared to that of peptide **1** indicating the importance of the presence of the thiol group in the peptide to replace the octanethiol ligand from the Au nano particle.

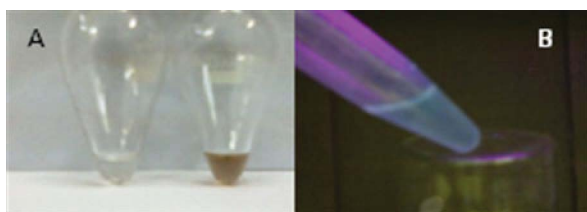


**Fig. 2** A: Comparison of peptide **4** (left) and **1** (right) attached Au nano particle solution in H<sub>2</sub>O; B: Fluorescent peptide **1** attached Au nano particles.

The peptide **1** attached gold solution was also found to be fluorescent around ~310 nm giving blue coloration (Fig. 2B) of the solution (but the solution of unattached peptide is nonfluorescent).

This made us assume that our peptides attached to Au nanoparticles could be detected through TEM or by fluorescence. The UV and fluorescent patterns of peptide **1** and its conjugate were studied next.

From the data it was evident that due to the attachment of the peptide **1** to AuNP, a red shift occurred showing a maxima at 260 nm. So, the fluorescence emission experiments were carried out at 260 nm excitation. From Fig. 3B it was clear that our gold nano conjugates were fluorescent in contrast to their unattached counterpart that showed a straight flattened line and the maxima of the fluorescent emission was at 312 nm with an excitation of 260 nm. That the maximum emission of the Au nano conjugate was at 260 nm was also supported by the emission Fig. 4A at different excitations.

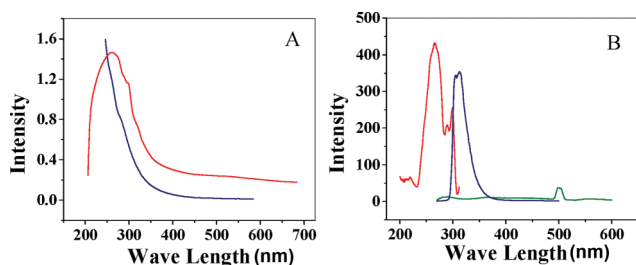


**Fig. 3** A: UV spectra of peptide **1** (blue) and **1** + AuNP (red); B: Fluorescence excitation of Peptide **1** (green) and **1**+AuNP (red) and emission spectra of **1**+AuNP (blue).

Next we applied our peptides and their corresponding Au nano conjugates to different bacteria and we found bactericidal activity of the peptides against two Gram (+) and Gram (-) bacteria. All

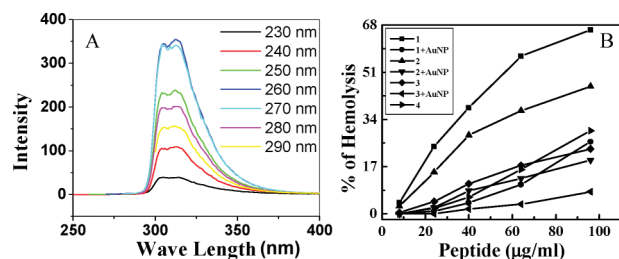


**Fig. 4** A: Comparison of the emission spectra of peptide **1**+AuNP at different excitation wave lengths; B: Hemolytic activity of the peptides against hRBC.

**Table 1**

Peptides	MIC Values of AuNP attached and their corresponding non-tagged peptides ( $\mu\text{g mL}^{-1}$ )			
	<i>S. aureus</i>	<i>B. subtilis</i>	<i>E. coli</i>	<i>P. aeruginosa</i>
1	19 $\pm$ 0.6	13 $\pm$ 0.4	19 $\pm$ 0.4	29 $\pm$ 0.8
1 + AuNP	22 $\pm$ 0.6	14 $\pm$ 0.4	22 $\pm$ 0.6	34 $\pm$ 0.8
2	3 $\pm$ 0.3	5 $\pm$ 0.3	14 $\pm$ 0.4	43 $\pm$ 0.7
2 + AuNP	5 $\pm$ 0.4	7 $\pm$ 0.4	16 $\pm$ 0.4	43 $\pm$ 0.8
3	24 $\pm$ 0.6	30 $\pm$ 0.6	37 $\pm$ 0.6	74 $\pm$ 0.8
3 + AuNP	43 $\pm$ 0.6	49 $\pm$ 0.6	43 $\pm$ 0.8	74 $\pm$ 0.8
4	22 $\pm$ 0.5	ND	24 $\pm$ 0.5	ND

the peptides showed moderate bactericidal activities against both kinds of bacteria shown in Table 1. However, it is to be noticed that **2** and its gold labeled analogue exhibited significant efficacy against the selected Gram (+) ve bacteria.

Also the data suggested that labeling of these peptides by gold did not significantly alter the bactericidal activities of these peptides. Cytotoxicities of these peptides and their gold labeled versions were determined by examining their hemolytic activity against hRBCs as reported by others also.

Peptide **1** showed the maximum hemolytic activity against hRBCs indicating its highest cytotoxicity among these peptides. Peptide **2** also showed significant cytotoxicity. The other peptides as indicated from the Fig. 4B showed much lower cytotoxicity against hRBCs. Interestingly the gold labeled versions of each of these peptides exhibited significantly lower hemolytic activity as compared to their unlabeled version. Particularly, the gold labeled versions of **1** and **2** showed approximately one third the hemolytic activity of their parent peptide. Altogether, the results indicated that gold labeling of the peptides generated only a marginal decrease in their bactericidal activities; however it significantly reduced their cytotoxic activities.

To understand the plausible mechanism of action, peptide-induced depolarization of hRBCs and *S. aureus* was assayed. A particular concentration of each of the peptides in their activity range was used to determine their ability to depolarize hRBC and *S. aureus* membrane. Fig. 5A indicates that **1** induced the maximum depolarization of hRBCs followed by **2** and other peptides. The gold labeled versions of the peptides induced much lower depolarization of hRBC membrane. The membrane depolarization data of the peptides showed a nice correlation with their hemolytic activity. Similarly, peptide-induced depolarization of *S. aureus* has been presented in Fig. 5B. **2** and its gold labeled analogue exhibited the highest membrane depolarization in

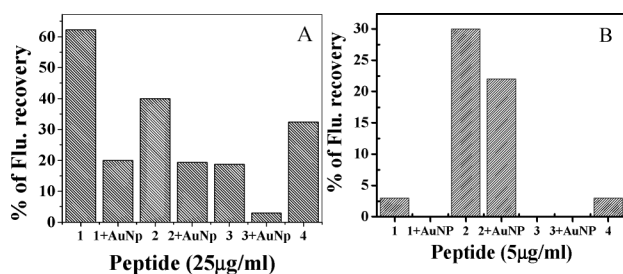


**Fig. 5** A. Percentage of fluorescence recovery hRBC membrane depolarization at 25 µg mL<sup>-1</sup>; B. Percentage of fluorescence recovery bacterial membrane depolarization at 5 µg mL<sup>-1</sup>.

*S. aureus*, however other peptides showed much lower activity at this concentration. It is to be pointed out that **2** also showed the highest bactericidal activity against *S. aureus* and the MIC value of **2** against this bacterium was significantly lower than the other peptides. Probably therefore, depolarization of *S. aureus* by other peptides at the MIC of **2** was significantly much lower. Thus a correlation was observed between the peptide-induced depolarization of *S. aureus* membrane and the relative bactericidal activity of the peptides indicating the cell membrane of the bacteria could be the potential target of these peptides. This was further strengthened by the electron micrographs which showed membrane perturbation of bacteria by each of the peptides at their MICs and sub-MICs. As seen in the TEM, the membrane budding caused by the peptide is clearly visible. Antibacterial activity of peptide **1** (both tagged and untagged) was confirmed by studying the bacterial morphology by the negative staining (1% aq. PTA pH adjusted to 7) TEM technique. Control *E. coli* ATCC10536 showed healthy morphology (Fig. 6A). Distinct cell membrane damage was observed in the form of blisters and protruding bubbles (indicated by arrow heads in Fig. 6B & C) on the bacterial membranes at the initial stages (below MIC treatment). Extensive membrane damage leading to cell lysis was observed at the MIC (Fig. 6D and E). Overall cell shrinkage was noted in affected cells. It appears that AuNP tagged and untagged peptide both alters bacterial morphology in a similar manner. It seems that the peptide mediates its antimicrobial activity by perforating the bacterial membrane followed by the efflux of cytoplasmic content finally resulting in bacterial death.

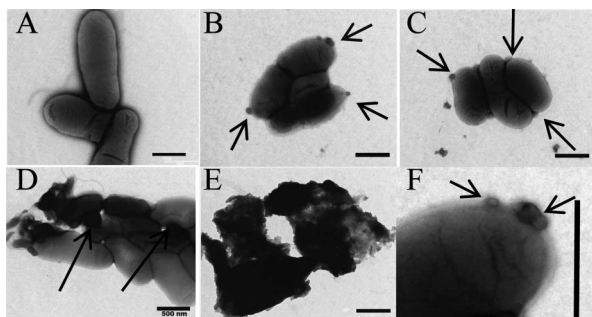


**Fig. 6** TEM of negatively stained (A) control *E. coli*; (B) *E. coli* + peptide **1** at 75% MIC; (C) *E. coli* + peptide **1** + AuNP at 75% MIC; (D) *E. coli* + peptide **1** at MIC; (E) *E. coli* + peptide **1** + AuNP at MIC; (F) blisters on bacteria shown in B at 80 kV. Bar represents 500 nm.

## Experimental

### General considerations

Oxygen and moisture-sensitive reactions were carried out in flame or oven-dried glassware sealed with rubber septa under dry nitrogen atmosphere. Similarly, sensitive liquids and solutions were transferred using a gas-tight syringe and cannula. Reagents were purchased and used without purification. Solvents were purified and dried following the usual procedures. Reactions were monitored by thin layer chromatography (TLC) carried out on 0.25 mm silica gel plates with UV light, I<sub>2</sub>, 7% ethanolic phosphomolybdic acid–heat and 2.5% ethanolic anisaldehyde (with 1% AcOH and 3.3% conc. H<sub>2</sub>SO<sub>4</sub>)–heat as developing agents. Silica gels of 60–120 and 200–300 mesh were used for chromatographic separation. <sup>1</sup>H NMR spectra are reported in ppm using TMS (0.00 ppm) or solvent (DMSO-*d*<sub>6</sub>; 2.50 ppm) as internal standard in 400 MHz instruments at 30 °C. Line broadening did not allow determination of any coupling constants. TOCSY experiments were carried out for all four compounds to assign the chemical shifts. Mass spectra were obtained under electron spray ionization (ESI) and high resolution mass spectrometer (HRMS-ESI) techniques. UV measurements were recorded in Thermo Evolution 600PC+ Vision UV spectrophotometer and fluorescence is measured in Varian Cary Eclipse Fluorescence Spectrophotometer.

### General procedure for EDCI and HOBt coupling

To a stirring solution of RCO-Lys(Boc)-OMe (0.1 mmol) in THF3 : MeOH3 : H<sub>2</sub>O (3 : 1 : 1; 5 mL) at 0 °C, LiOH·H<sub>2</sub>O (12.6 mg, 0.3 mmol) was added and stirred at room temperature for 1 h. The reaction mixture was then acidified to pH 2 with 1 N HCl. The reaction mixture was extracted with EtOAc (2 × 50 mL). The combined organic extracts were washed with water (50 mL), brine (50 mL), dried (Na<sub>2</sub>SO<sub>4</sub>), filtered and concentrated *in vacuo* to get the acid. The crude acid was used for the next reaction without further purification.

To a stirred solution of *cyclo*-[Saa(BocNH)-Phe-Leu]<sub>2</sub> (0.1 mmol) in dry dichloromethane (3 mL) at 0 °C was added trifluoroacetic acid (1.5 mL) and stirred for 2 h at room temperature. The reaction mixture was then concentrated *in vacuo* to get the trifluoroacetate salt.

To a stirring solution of the crude acid in dry dichloromethane (3 mL) at 0 °C was sequentially added HOBt·H<sub>2</sub>O (21 mg, 0.15 mmol) and EDCI (29 mg, 0.15 mmol). After 10 min, the above-prepared trifluoroacetate salt was dissolved in dichloromethane (3 mL) and added to the reaction mixture followed by the addition of DIPEA (0.09 mL, 0.5 mmol). After stirring for 12 h at room temperature, the reaction mixture was diluted with EtOAc (50 mL), washed with 1 N HCl solution (2 × 10 mL), saturated NaHCO<sub>3</sub> solution (2 × 10 mL), water (10 mL), brine (10 mL), dried (Na<sub>2</sub>SO<sub>4</sub>), filtered and concentrated *in vacuo*. The residue was purified by chromatography to afford the pure compound.

### General procedure for the preparation of final compounds

To a stirred solution of *cyclo*-[Saa(RCO-Lys(Boc)NH)-Phe-Leu]<sub>2</sub> (0.1 mmol) in dry dichloromethane (3 mL) at 0 °C was added trifluoroacetic acid (1.5 mL) and stirred for 2 h at room

temperature. The reaction mixture was then concentrated *in vacuo* to get trifluoroacetate salt. The compound was then dissolved in the minimum volume of TFA and transferred to 10 mL of dry ether solution and centrifuged at 8000 rpm for 15 min. The solution was decanted and the solid was again vortexed with 10% chloroform in dry ether solution. The mixture was again centrifuged and the upper solution was decanted. The washing was repeated for three times to get pure compound.

**Data for 1.**  $^1\text{H NMR}$  (400 MHz,  $\text{DMSO-}d_6$ ):  $\delta$  7.32–7.21 (phenyl, 5H), 8.89 (LeuNH, 1H), 8.46 (PheNH, 1H), 8.07 (SaaNH, 1H), 7.99 (LysNH, 1H), 7.70 (Lys  $\epsilon$ NH, 1H), 7.26 (Saa  $\gamma$ NH, 1H), 4.45 (PheC $_{\alpha}$ H, 1H), 4.36 (SaaC $_{\alpha}$ H, 1H), 4.21 (LysC $_{\alpha}$ H, 1H), 3.96 (SaaC $_{\delta}$ H, 1H), 3.61 (SaaC $_{\gamma}$ H, 1H), 3.48 (LeuC $_{\alpha}$ H, 1H), 3.41 (PheC $_{\beta}$ H, 1H), 3.11 (PheC $_{\beta'}$ H, 1H), 2.89 (CH $_2$ SH, 2H), 2.78 (LysC $_{\epsilon/\epsilon'}$ H, 2H), 2.54 (CH $_2$ CH $_2$ SH), 2.42 (SaaC $_{\epsilon/\epsilon'}$ H, 2H), 1.71 (LeuC $_{\beta/\beta'}$ H, 2H), 1.66 (SaaC $_{\beta/\beta'}$ H, 2H), 1.65 (LysC $_{\beta/\beta'}$ H, 2H), 1.57 (LeuC $_{\gamma}$ H, 1H), 1.52 (LysC $_{\delta/\delta'}$ H, 2H), 1.34 (LysC $_{\gamma/\gamma'}$ H, 2H), 0.87 (LeuC $_{\delta/\delta'}$ H, 6H); MS (ESI):  $m/z$  1238 [M + 2H] $^+$ , 620 [M/2 + H] $^+$ ; HRMS (ESI): calcd. for C $_{60}$ H $_{94}$ N $_{12}$ O $_{12}$ S $_2$  [M/2 + H] $^+$  619.3252, found 619.3272

**Data for 2.**  $^1\text{H NMR}$  (400 MHz,  $\text{DMSO-}d_6$ ):  $\delta$  7.32–7.21 (phenyl, 5H), 8.20 (LeuNH, 1H), 8.07 (SaaNH, 1H), 8.00 (PheNH, 1H), 7.94 (LysNH, 1H), 7.66 (Saa  $\gamma$ NH, 1H), 7.64 (Lys  $\epsilon$ NH, 1H), 4.58 (PheC $_{\alpha}$ H, 1H), 4.52 (LeuC $_{\alpha}$ H, 1H), 4.35 (SaaC $_{\alpha}$ H, 1H), 4.17 (LysC $_{\alpha}$ H, 1H), 3.98 (SaaC $_{\delta}$ H, 1H), 3.21 (SaaC $_{\gamma}$ H, 1H), 3.15 (PheC $_{\beta}$ H, 1H), 2.98 (PheC $_{\beta'}$ H, 1H), 2.89 (CH $_2$ SH, 2H), 2.76 (LysC $_{\epsilon/\epsilon'}$ H, 2H), 2.54 (CH $_2$ CH $_2$ SH), 1.98 (SaaC $_{\epsilon/\epsilon'}$ H, 2H), 1.59 (LeuC $_{\beta/\beta'}$ H, 2H), 1.57 (LysC $_{\beta/\beta'}$ H, 2H), 1.53 (LysC $_{\delta/\delta'}$ H, 2H), 1.40 (LeuC $_{\gamma}$ H, 1H), 1.28 (LysC $_{\gamma/\gamma'}$ H, 2H), 0.82 (LeuC $_{\delta/\delta'}$ H, 6H); HRMS (ESI): calcd. for C $_{60}$ H $_{92}$ N $_{12}$ O $_{12}$ S $_2$  [M] $^+$  1236.6399, found 1236.6335

**Data for 3.**  $^1\text{H NMR}$  (400 MHz,  $\text{DMSO-}d_6$ ):  $\delta$  7.32–7.25 (phenyl, 5H), 8.92 (LeuNH, 1H), 8.46 (PheNH, 1H), 8.08 (SaaNH, 1H), 7.86 (LysNH, 1H), 7.66 (Lys  $\epsilon$ NH, 1H), 7.26 (Saa  $\gamma$ NH, 1H), 4.44 (PheC $_{\alpha}$ H, 1H), 4.35 (SaaC $_{\alpha}$ H, 1H), 4.19 (LysC $_{\alpha}$ H, 1H), 3.95 (SaaC $_{\delta}$ H, 1H), 3.55 (SaaC $_{\gamma}$ H, 1H), 3.42 (LeuC $_{\alpha}$ H, 1H), 3.40 (PheC $_{\beta}$ H, 1H), 3.08 (PheC $_{\beta'}$ H, 1H), 3.08 (CH $_2$ CH $_2$ CH $_2$ CH $_2$ CH $_2$ SH), 2.76 (LysC $_{\epsilon/\epsilon'}$ H, 2H), 2.43 (SaaC $_{\epsilon/\epsilon'}$ H, 2H), 2.12 (CH $_2$ CH $_2$ CH $_2$ CH $_2$ CH $_2$ SH), 1.69 (LeuC $_{\gamma}$ H, 1H), 1.68 (CH $_2$ CH $_2$ CH $_2$ CH $_2$ CH $_2$ SH), 1.66 (SaaC $_{\beta/\beta'}$ H, 2H), 1.60 (LysC $_{\beta/\beta'}$ H, 2H), 1.52 (LeuC $_{\beta/\beta'}$ H, 2H), 1.50 (CH $_2$ CH $_2$ CH $_2$ CH $_2$ CH $_2$ SH), 1.50 (LysC $_{\delta/\delta'}$ H, 2H), 1.35 (CH $_2$ CH $_2$ CH $_2$ CH $_2$ CH $_2$ SH), 1.31 (LysC $_{\gamma/\gamma'}$ H, 2H), 0.78 (LeuC $_{\delta/\delta'}$ H, 3H); 0.64 (LeuC $_{\delta/\delta'}$ H, 3H); MS (ESI):  $m/z$  1320 [M] $^+$ , 1167 [M – 2 × C $_4$ H $_8$ S + Na] $^+$ ; HRMS (ESI): calcd. for C $_{66}$ H $_{104}$ N $_{12}$ O $_{12}$ S $_2$  [M – 2 × C $_4$ H $_8$ S + Na] $^+$  1167.6644, found 1167.6367

**Data for 4.**  $^1\text{H NMR}$  (400 MHz,  $\text{DMSO-}d_6$ ):  $\delta$  7.33–7.22 (phenyl, 5H), 8.92 (LeuNH, 1H), 8.46 (PheNH, 1H), 8.11 (SaaNH, 1H), 7.86 (LysNH, 1H), 7.66 (Lys  $\epsilon$ NH, 1H), 7.28 (Saa  $\gamma$ NH, 1H), 4.44 (PheC $_{\alpha}$ H, 1H), 4.37 (SaaC $_{\alpha}$ H, 1H), 4.19 (LysC $_{\alpha}$ H, 1H), 3.96 (SaaC $_{\delta}$ H, 1H), 3.55 (SaaC $_{\gamma}$ H, 1H), 3.43 (LeuC $_{\alpha}$ H, 1H), 3.41 (PheC $_{\beta}$ H, 1H), 3.08 (PheC $_{\beta'}$ H, 1H), 2.77 (LysC $_{\epsilon/\epsilon'}$ H, 2H), 2.44 (SaaC $_{\epsilon/\epsilon'}$ H, 2H), 2.13 (CH $_2$ , 2H), 1.69 (LeuC $_{\gamma}$ H, 1H), 1.66 (SaaC $_{\beta/\beta'}$ H, 2H), 1.60 (LysC $_{\beta/\beta'}$ H, 2H), 1.52 (LeuC $_{\beta/\beta'}$ H, 2H), 1.50 (LysC $_{\delta/\delta'}$ H, 2H), 1.31 (LysC $_{\gamma/\gamma'}$ H, 2H), 0.97 (CH $_3$ , 3H), 0.78 (LeuC $_{\delta/\delta'}$ H, 3H); 0.64 (LeuC $_{\delta/\delta'}$ H, 3H); HRMS (ESI): calcd. for C $_{60}$ H $_{92}$ N $_{12}$ O $_{12}$  [M + H] $^+$  1173.6958, found 1173.7051.

## Hemolytic activity assay of the peptides

Hemolytic activity of the peptides against human red blood cells (hRBCs) in PBS was examined to check their cytotoxicity by a standard procedure <sup>9,10</sup> In brief, fresh hRBCs, collected in the presence of an anti-coagulant from a healthy volunteer, were washed three times in PBS. Freshly dissolved peptides in water at the desired concentrations were added to the suspension of red blood cells (6% final in v/v) in PBS to the final volume of 200  $\mu\text{L}$  and incubated at 37 °C for 35 min. The samples were then centrifuged for 10 min at 2000 r.p.m. and the release of hemoglobin was determined by measuring the absorbance ( $A_{\text{sample}}$ ) of the supernatant at 540 nm. Absorbance of hRBC in PBS ( $A_{\text{blank}}$ ) and in 0.2% (final concentration v/v) Triton X-100 ( $A_{\text{triton}}$ ) were used as negative and positive controls respectively. The percentage of hemolysis was calculated according to the following equation.

$$\text{Percentage of hemolysis} = [(A_{\text{sample}} - A_{\text{blank}})/(A_{\text{triton}} - A_{\text{blank}})] \times 100$$

## Detection of antibacterial activity of the peptides

The antibacterial activity of the peptides was assayed in a sterile 96 well plate in 100  $\mu\text{L}$  final volume under aerobic conditions. In brief, mid-log phase bacteria were washed thrice by PBS and re-suspended as such to gain nearly 10<sup>5</sup> CFU per ml. 50  $\mu\text{L}$  bacterial suspension, with 10<sup>5</sup> CFU per ml were added to 50  $\mu\text{L}$  of water containing two fold serially diluted different peptides in each well and incubated for 3 h at 37 °C. After three hour incubation, the bacterial suspension was diluted 100 times with PBS. Then 10  $\mu\text{L}$  of each diluted suspension was spotted onto an LB agar plate employing a multichannel pipette. The plates were incubated at 37 °C for 18–24 h. The antibacterial activity of the peptides was expressed in terms of their MICs which indicate the peptide concentrations that result in the 100% inhibition of microbial growth as observed from the absence of any visible bacterial colony. The microorganisms used were Gram-positive bacteria, *Bacillus subtilis* ATCC 6633 and *Staphylococcus aureus* ATCC 9144 and Gram-negative bacterium, *Escherichia coli* ATCC 10536 and *Pseudomonas aurogenosa*.

## Detection of peptide-induced depolarization of hRBC and *S. aureus* cell membrane

Peptide-induced depolarization of the hRBC and *S. aureus* membrane was detected by its efficacy to dissipate the potential across these cell membranes.<sup>11</sup> Fresh hRBCs, collected similarly to the hemolytic activity assay experiments were re-suspended in PBS buffer with a final cell volume of 0.6% (v/v). The bacteria were grown at 37 °C until they reached to their midlog phase and centrifuged followed by washing with buffer (20 mM glucose, 5 mM HEPES, pH 7.3). Then bacteria were re-suspended (final  $\sim 2 \times 10^5$  CFU per mL) in the similar buffer containing 0.1 M KCl. Both hRBCs and bacteria were incubated with diS-C3-5 probe for 1 h. When the fluorescence level (excitation and emission wavelengths set at 620 and 670 nm, respectively) of the hRBCs or bacterial suspension became stable, different amounts of each of the peptides were added to these suspensions in order to record the peptide-induced membrane depolarization of either hRBCs or bacterial membrane. Membrane depolarization as measured by the fluorescence recovery ( $F_r$ ) was defined by the equation<sup>12</sup>

$$F_t = [(I_t - I_0)/(I_f - I_0)] \times 100\%$$

Where  $I_t$ , the total fluorescence, was the fluorescence levels of cell suspensions just after the addition of diS-C<sub>3</sub>-5;  $I_t$ , was the observed fluorescence after the addition of a peptide at a particular concentration either to hRBCs, or to *S. aureus* suspensions, which were already incubated with diS-C<sub>3</sub>-5 probe for 1 h and  $I_0$ , was the steady-state fluorescence level of the cell suspensions after 1 h incubation with the probe.

### TEM Characterization of nano-gold tagged peptide (in MeOH & in water)

A 7  $\mu$ L sample was allowed to adsorb on pioloform or carbon coated copper grids (400 mesh) held between tweezers and excess solution was blotted off with a filter paper. The grids were air dried and observed at 265 000 $\times$  under a FEI Tecnai 12 Twin Transmission electron microscope operating at 120 kV equipped with a MegaView II CCD camera. Analysis was done using analySIS software (Soft Imaging Systems, Herzogenrath Germany).

### Morphological alterations of *E. coli* on treatment with anti-bacterial peptide (using TEM)

*E. coli* after treatment with anti-bacterial peptide was centrifuged and the pellet was washed in Tris Buffer pH7 followed by another centrifugation step. The pellet was finally re-suspended in 100  $\mu$ L Tris Buffer. Pioloform coated copper grids were prepared and glow discharged to make the substrate hydrophilic. A 7  $\mu$ L sample was deposited onto these grids and allowed to adsorb for 2 min. Excess solution was removed by placing a filter paper at the edge of the grid. The grids were then washed with triple distilled water and negatively stained<sup>13</sup> with 1% phosphotungstic acid (pH adjusted to 7) and air dried. Grids were then analyzed under a Philips FEI Tecnai 12 Twin Transmission Electron Microscope at 80 kV. Images were acquired at 21 000 $\times$  using a MegaView II CCD camera and analyzed using analySIS software.

### Conclusions

In conclusion, our initial studies indicate that attachment of AuNP to our peptides does not change the antimicrobial activity too much but the cytotoxicities of the peptides were decreased significantly. And the thiol group is not only necessary for the attachment of our peptide to AuNP but also for the broad spectrum activity of the peptides as reflected in Table 1. Our studies through TEM and peptide induced depolarisation indicated a membrane perturbing mechanistic pathway of the peptides giving an initial insight into the mechanistic aspect.

### Acknowledgements

Authors acknowledge SAIF, CDRI for spectroscopic and analytical data. S.P. is thankful to CSIR, New Delhi for research fellowship.

### Notes and references

- 1 L. M. Jarvis, *Chem. Eng. News*, 2010, **88**, 30.
- 2 (a) R. Karstad, G. Isaksen, B.-O. Brandsdal, J. S. Svendsen and J. Svenson, *J. Med. Chem.*, 2010, **53**, 5558; (b) T. Hansen, T. Alst, M. Havelkova and M. B. Ström, *J. Med. Chem.*, 2009, **52**, 595; (c) H. A. Pereira, *Curr. Pharm. Biotechnol.*, 2006, **7**, 229; (d) K. L. Brown and R. E. W. Hancock, *Curr. Opin. Immunol.*, 2006, **18**, 24; (e) M. Zasloff, *Nature*, 2002, **415**, 389; (f) R. E. W. Hancock and R. Lehrer, *TIBTECH*, 1998, **16**, 82.
- 3 (a) R. M. Epand, S. Rotem, A. Mor, B. Berno and R. F. Epand, *J. Am. Chem. Soc.*, 2008, **130**, 14346; (b) A. A. Langham, A. S. Ahmad and Y. N. Kaznessis, *J. Am. Chem. Soc.*, 2008, **130**, 4338; (c) H. Leontiadou, A. E. Mark and S. J. Marrink, *J. Am. Chem. Soc.*, 2006, **128**, 12156; (d) S. K. Straus and R. E. W. Hancock, *Biochim. Biophys. Acta, Biomembr.*, 2006, **1758**, 1215; (e) B. L. Kagan and M. E. Selsted, *Proc. Natl. Acad. Sci. U. S. A.*, 1990, **87**, 210; (f) B. Christensen, J. Fink, R. B. Merrifield and D. Mauzerall, *Proc. Natl. Acad. Sci. U. S. A.*, 1988, **85**, 5072.
- 4 (a) Y. Zhao, Y. Tian, Y. Cui, W. Liu, W. Ma and X. Jiang, *J. Am. Chem. Soc.*, 2010, **132**, 12349; (b) S.-Y. Lin, N.-T. Chen, S.-P. Sum, L.-W. Lo and C.-S. Yang, *Chem. Commun.*, 2008, 4762; (c) A. G. Tkachenko, H. Xie, Y. Liu, D. Coleman, J. Ryan, W. R. Glomm, M. K. Shipton, S. Frazen and D. L. Feldheim, *Bioconjugate Chem.*, 2004, **15**, 482.
- 5 For reviews on sugar amino acids see: (a) M. D. P. Risseuw, M. Overhand, G. W. J. Fleet and M. I. Simone, *Tetrahedron: Asymmetry*, 2007, **18**, 2001; (b) K. J. Jensen and J. Brask, *J. Peptide Sci.*, 2005, **80**, 747; (c) T. K. Chakraborty, P. Srinivasu, S. Tapadar and B. K. Mohan, *Glycoconjugate J.*, 2005, **22**, 83; (d) T. K. Chakraborty, P. Srinivasu, S. Tapadar and B. K. Mohan, *J. Chem. Sci.*, 2004, **116**, 187; (e) S. A. W. Gruner, E. Locardi, E. Lohof and H. Kessler, *Chem. Rev.*, 2002, **102**, 491; (f) F. Schweizer, *Angew. Chem., Int. Ed.*, 2002, **41**, 230; (g) T. K. Chakraborty, S. Ghosh and S. Jayaprakash, *Curr. Med. Chem.*, 2002, **9**, 421; (h) T. K. Chakraborty, S. Jayaprakash and S. Ghosh, *Comb. Chem. High Throughput Screening*, 2002, **5**, 373; (i) F. Peri, L. Cipolla, E. Forni, B. La, Ferla and F. Nicotra, *Chemtracts: Org. Chem.*, 2001, **14**, 481; (j) J. Gervay-Hague and T. M. Weathers, *Pyranosyl Sugar Amino Acid Conjugates: Their Biological Origins, Synthetic Preparations And Structural Characterisation*, in *Glycochemistry: Principles, Synthesis and Applications*, P. G. Wang, ed.; Dekker Bertozzi, C. R. New York, 2001.
- 6 For some earlier works on sugar amino acid containing and other cyclic antimicrobial peptides see: (a) V. V. Kapoerchan, A. D. Knijnenburg, M. Niamat, E. Spalburg, A. J. de Neeling, P. H. Nibbering, R. H. Mars-Groenendijk, D. Noort, J. M. Otero, A. L. Llamas-Saiz, M. J. van Raaij, G. A. van der Marel, H. S. Overkleeft and M. Overhand, *Chem.-Eur. J.*, 2010, **16**, 12174 and the references cited therein; (b) M. Tamaki, I. Sasaki, M. Kokuno, M. Shindo, M. Kimura and Y. Uchida, *Org. Biomol. Chem.*, 2010, **8**, 1791; (c) T. K. Chakraborty, D. Koley, R. Rapolu, V. Krishnakumari, R. Nagaraj and A. C. Kunwar, *J. Org. Chem.*, 2008, **73**, 8731; (d) G. M. Grotenbreg, A. E. M. Buizert, A. L. Llamas-Saiz, E. Spalburg, P. A. V. van Hooft, A. J. de Neeling, D. Noort, M. J. van Raaij, G. A. van der Marel, H. S. Overkleeft and M. Overhand, *J. Am. Chem. Soc.*, 2006, **128**, 7559; (e) T. K. Chakraborty, S. Roy, D. Koley, S. K. Dutta and A. C. Kunwar, *J. Org. Chem.*, 2006, **71**, 6240; (f) J. Xiao, B. Weisblum and P. Wipf, *Org. Lett.*, 2006, **8**, 4731.
- 7 N. V. S. Kumar, P. Sharma, H. Singh, D. Koley, S. Roy and T. K. Chakraborty, *J. Phys. Org. Chem.*, 2010, **23**, 238.
- 8 F. Porta, G. Speranza, Z. Krpetic, V. D. Santo, P. Francescato and G. Scari, *Mater. Sci. Eng., B*, 2007, **140**, 187.
- 9 Z. Oren and Y. Shai, *Biochemistry*, 1997, **36**, 1826.
- 10 A. Ahmad, S. P. Yadav, N. Asthana, K. Mitra, S. P. Srivastava and J. K. Ghosh, *J. Biol. Chem.*, 2006, **281**, 22029.
- 11 N. Papo, A. Braunstein, Z. Eshhar and Y. Shai, *Cancer Res.*, 2004, **64**, 5779.
- 12 P. J. Sims, A. S. Waggoner, C. H. Wang and J. F. Hoffman, *Biochemistry*, 1974, 3315.
- 13 S. Brenner and R. W. Horne, *Biochim. Biophys. Acta*, 1959, **34**, 103.